Electronic Supplementary Information

Membrane nanotube pearling restricted by confined polymers

Zengshuai Yan,[a] Shixin Li,[b] Zhen Luo,[b] Yan Xu[b] and Tongtao Yue[a,b]

[a] *State Key Laboratory of Heavy Oil Processing, China University of Petroleum (East China), Qingdao 266580, China*

[b] *Center for Bioengineering and Biotechnology, College of Chemical Engineering, China University of Petroleum (East China), Qingdao 266580, China*

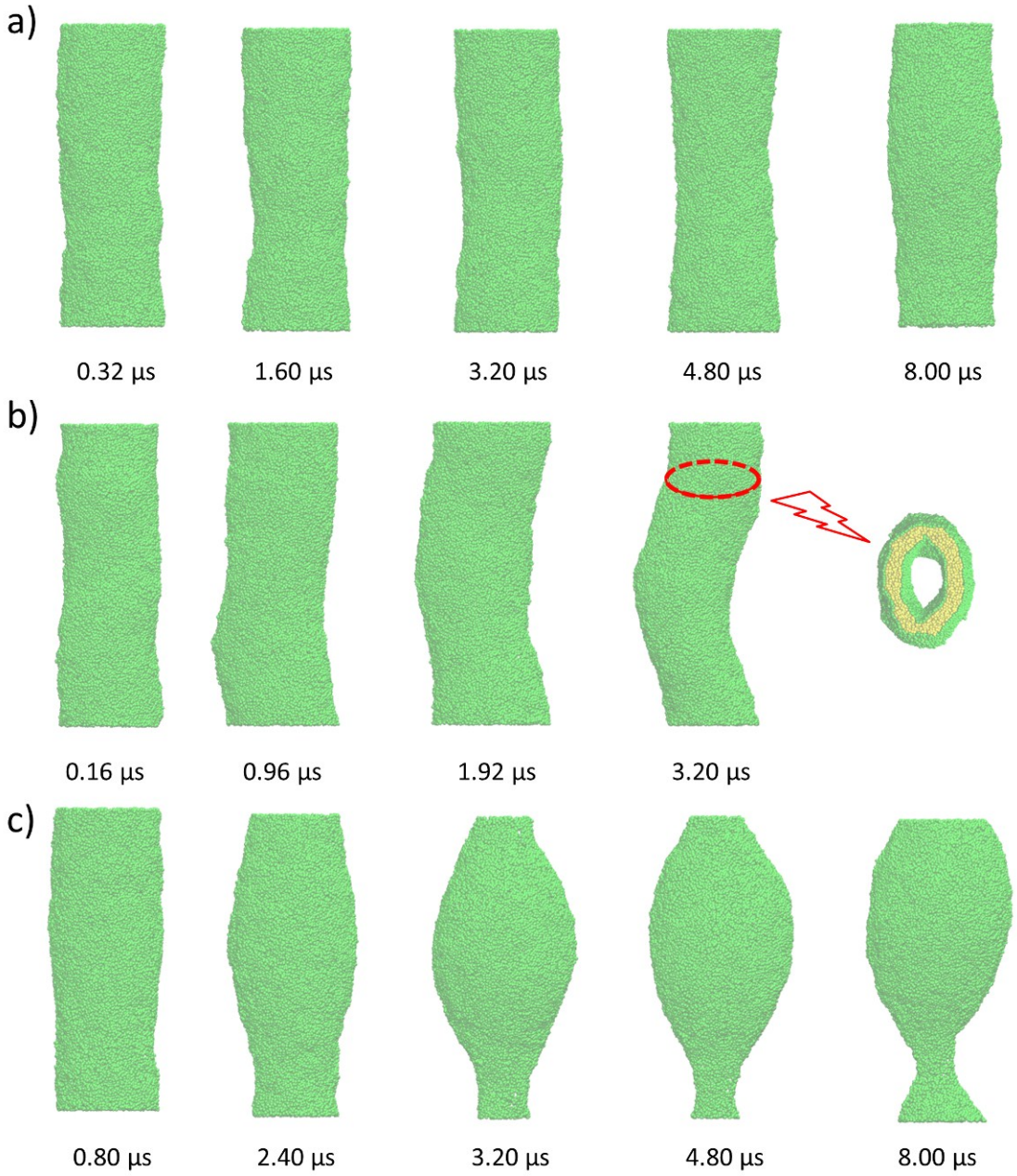

Fig. S1 Time sequences of typical snapshots depicting the morphological change of pure membrane nanotubes of different inner water pressures. The number of water beads inside the tubes are respectively, N_W = 51,000 (a), N_W = 41,000 (b) and N_W = 61,000 (c).

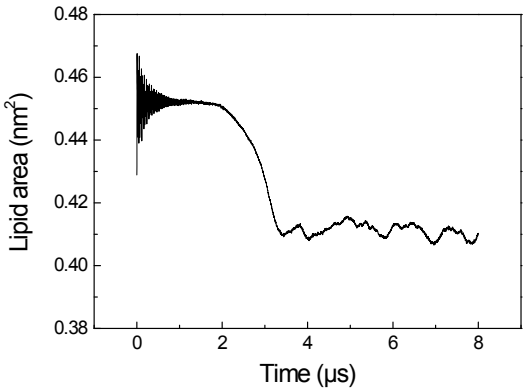

Fig. S2 Time evolution of the lipid area representing the nanotube pearling induced by the high membrane surface tension. The number of inner water beads was fixed at 61,000.

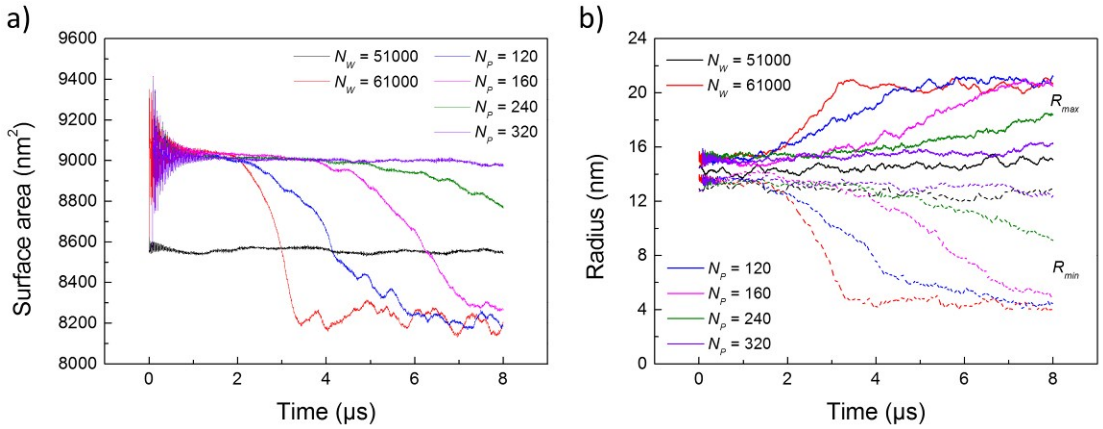

Fig. S3 The effect of the polymer concentration on the nanotube pearling. (a) Time evolutions of the surface area of nanotubes confining polymers of different concentrations. (b) Time evolutions of the maximal and minimal tube radii.

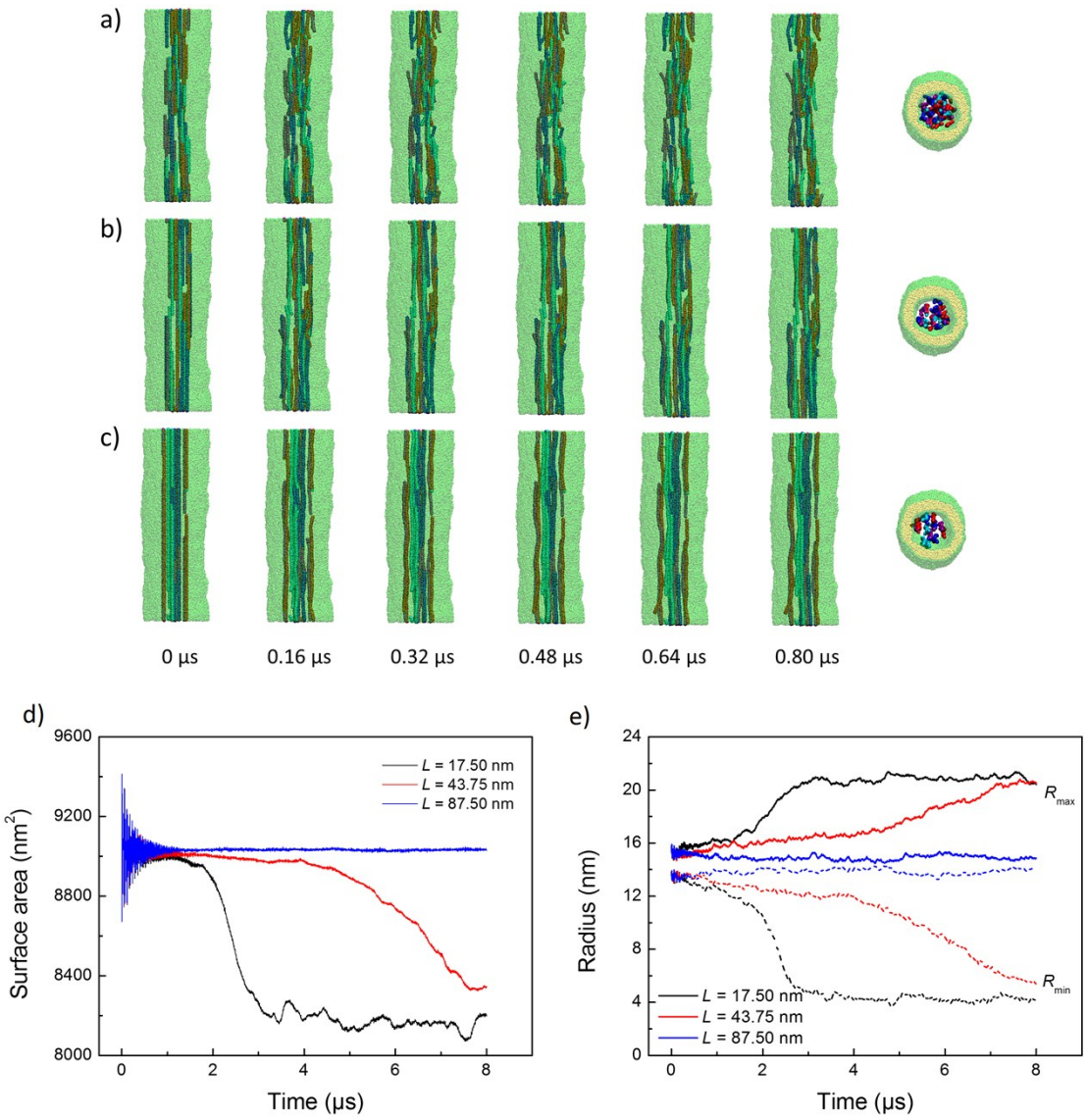

Fig. S4 The negligible effect of initial polymer configuration on the final simulation results. The time for the first equilibrium simulation during which lipids were restrained to move was increased from 10,000 steps to 50,000 steps. (a-c) Time sequences of typical snapshots showing equilibrium of polymers confined in nanotubes. (d) Time evolutions of the surface area of nanotubes confining polymers of three different lengths (L). (e) Time evolutions of both the maximal and the minimal radii of nanotubes. The total number of beads inside the nanotube was fixed as 61,000.

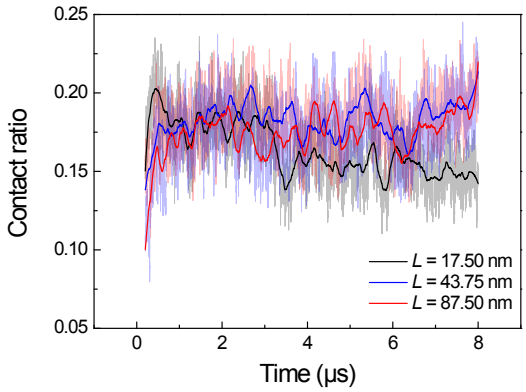

Fig. S5 Time evolutions of the contact ratio between polymers and lipids during restrained pearling of nanotubes confining polymers of different lengths.

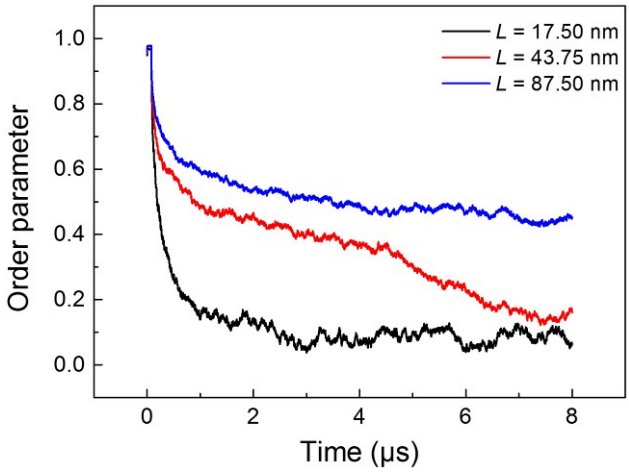

Fig. S6 Time evolutions of the order parameter of polymers of different lengths confined in nanotubes of $N_W = 61{,}000$.

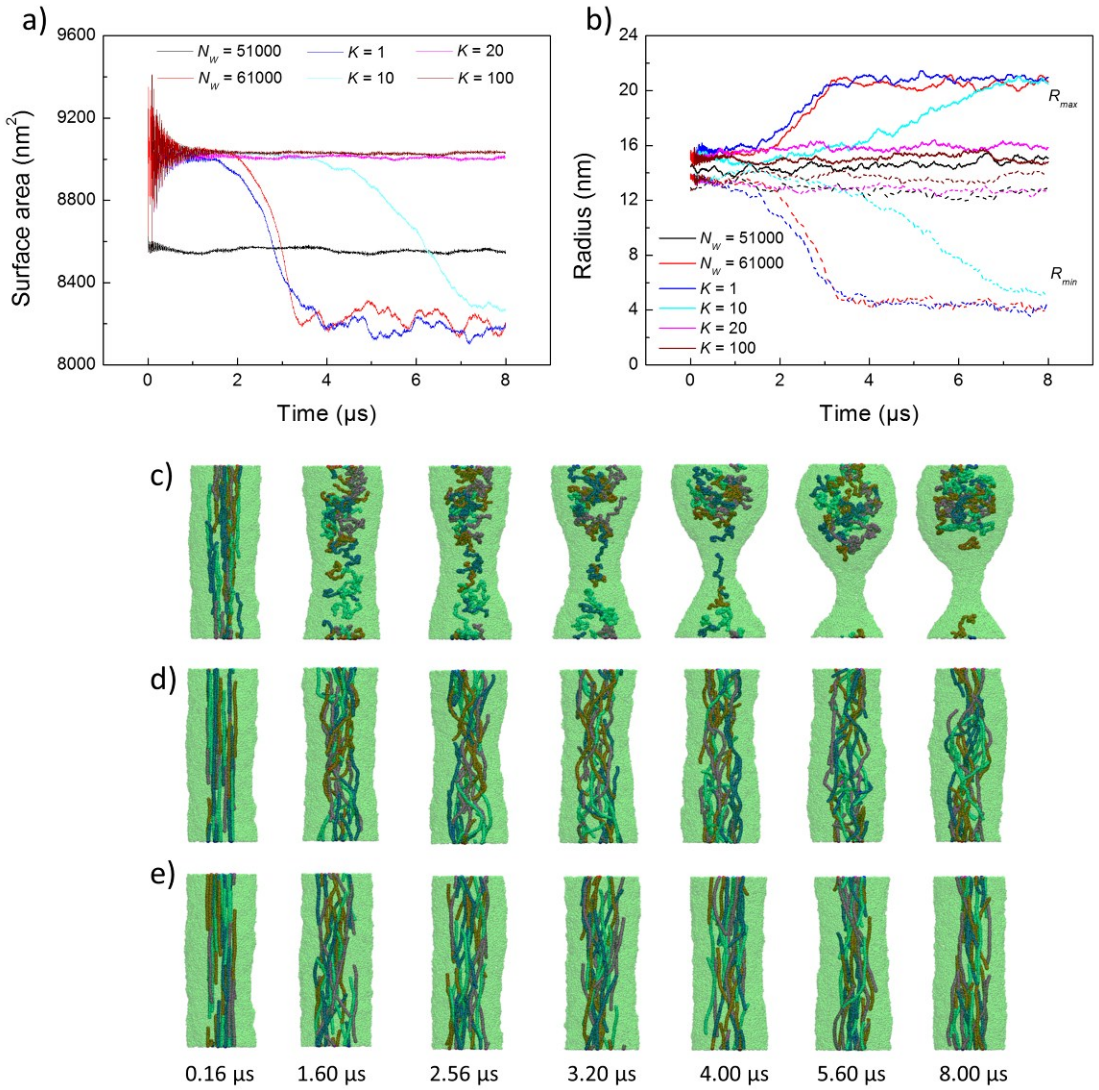

Fig. S7 The effect of the polymer bending stiffness on the nanotube pearling. (a) Time evolutions of the tube surface area. (b) Time evolutions of both the maximal and the minimal radii. (c-e) Time sequences of typical snapshots depicting morphological changes of nanotubes confining polymers of the same length but different stiffness: K = 1 (c), K = 20 (d), K = 100 (e).

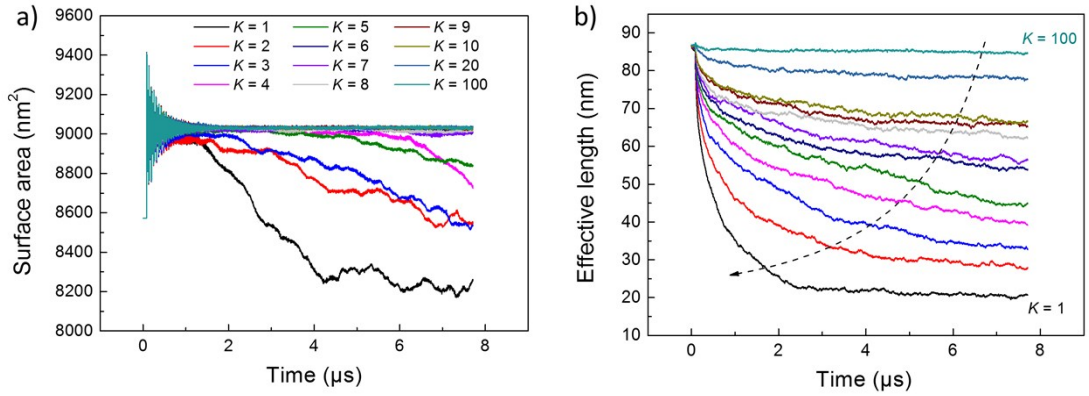

Fig. S8 Estimation of the critical polymer length below which the nanotube pearling can finally occur. (a) Time evolutions of the surface area of nanotubes confining polymer of different bending stiffness. (b) Time evolutions of the effective length of polymers confined in the nanotubes, which was calculated as the largest distance between two beads of a polymer.

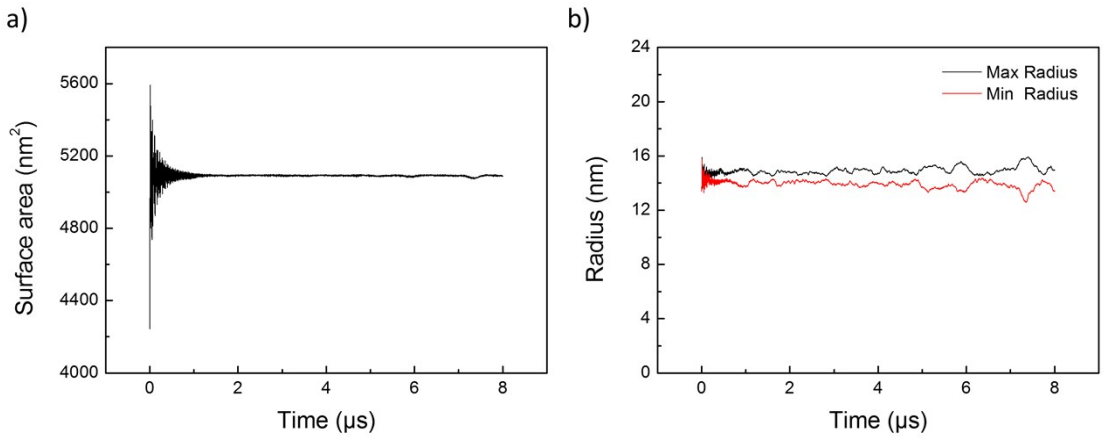

Fig. S9 Restrained pearling of a short nanotube of 75 nm under the same pressure difference between interior and exterior of the tube. (a) Time evolution of the tube surface area. (b) Time evolutions of both maximal and minimal tube radii.

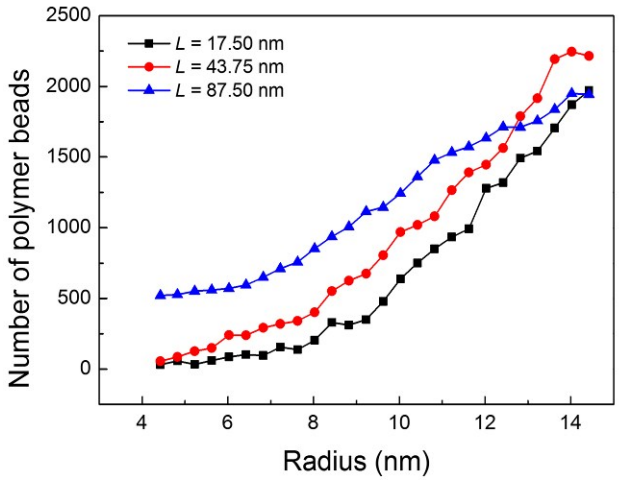

Fig. S10 The number of polymer beads locating at the tube shrinking region as the nanotube was enforced to undergo pearling.

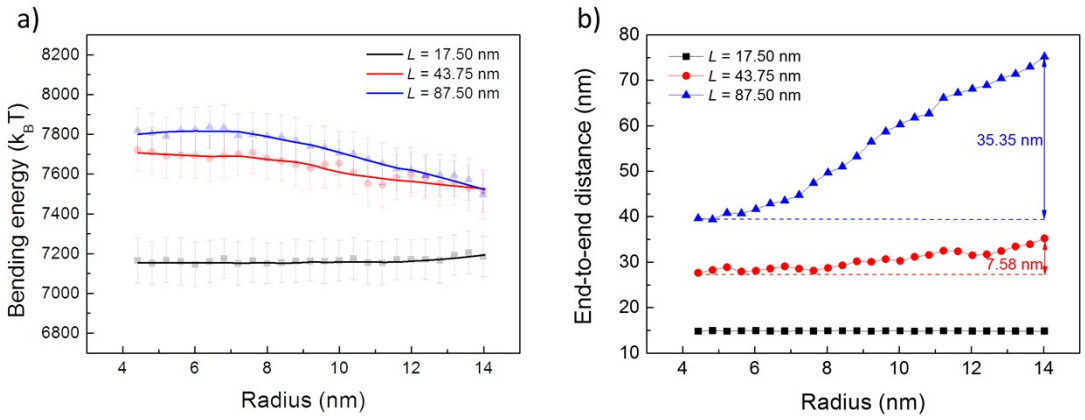

Fig. S11 The enforced nanotube pearling costing bending energies of confined polymers of different lengths. (a) The total bending energy of confined polymers as a function of the radius of middle tube region, on which the restraining force was exerted to guide the nanotube pearling. (b) The average end-to-end distance of confined polymers illustrating different extent of bending of confined polymers of different lengths.

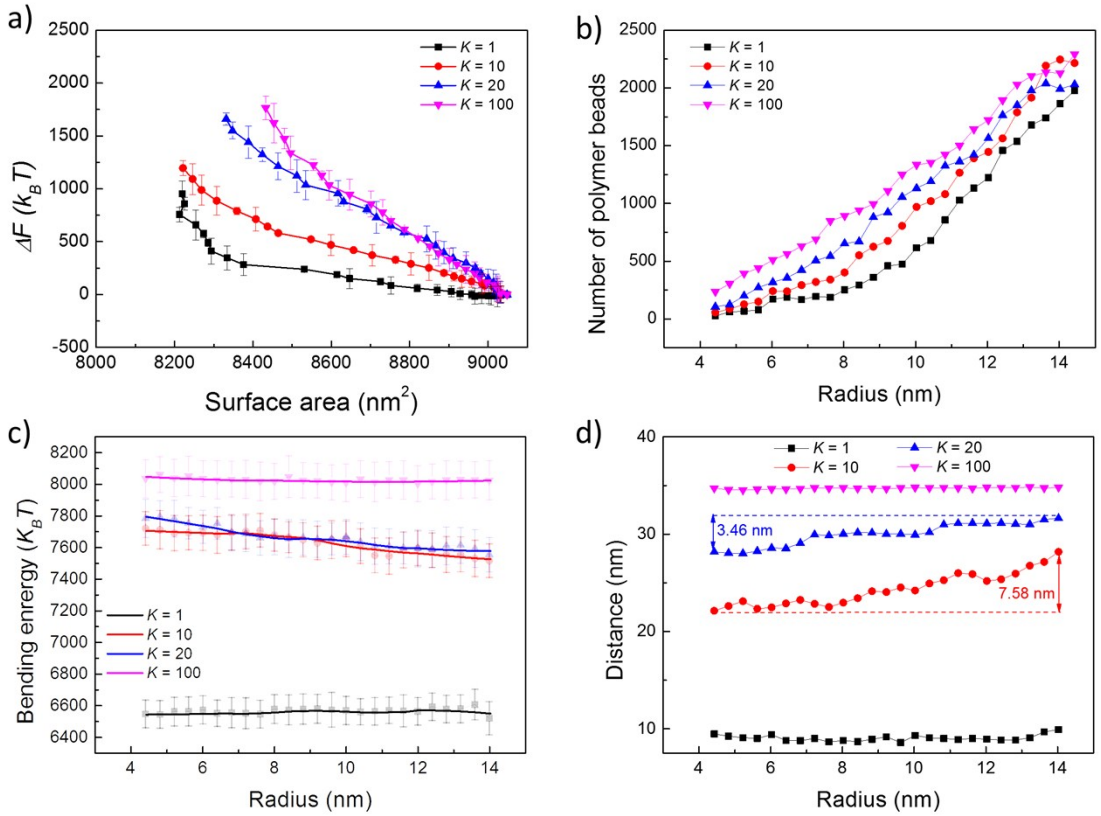

Fig. S12 Free energy analysis of the effect of the polymer bending stiffness on the nanotube pearling. (a) The system free energy change as a function of surface area of nanotubes confining polymers of L = 43.75 nm but different bending stiffness. (b) The number of polymer beads locating at the tube shrinking region. (c) The total bending energy of polymers as a function of the shrinking tube radius. (d) The average end-to-end distance of confined polymers of different bending stiffness as a function of the shrinking tube radius.

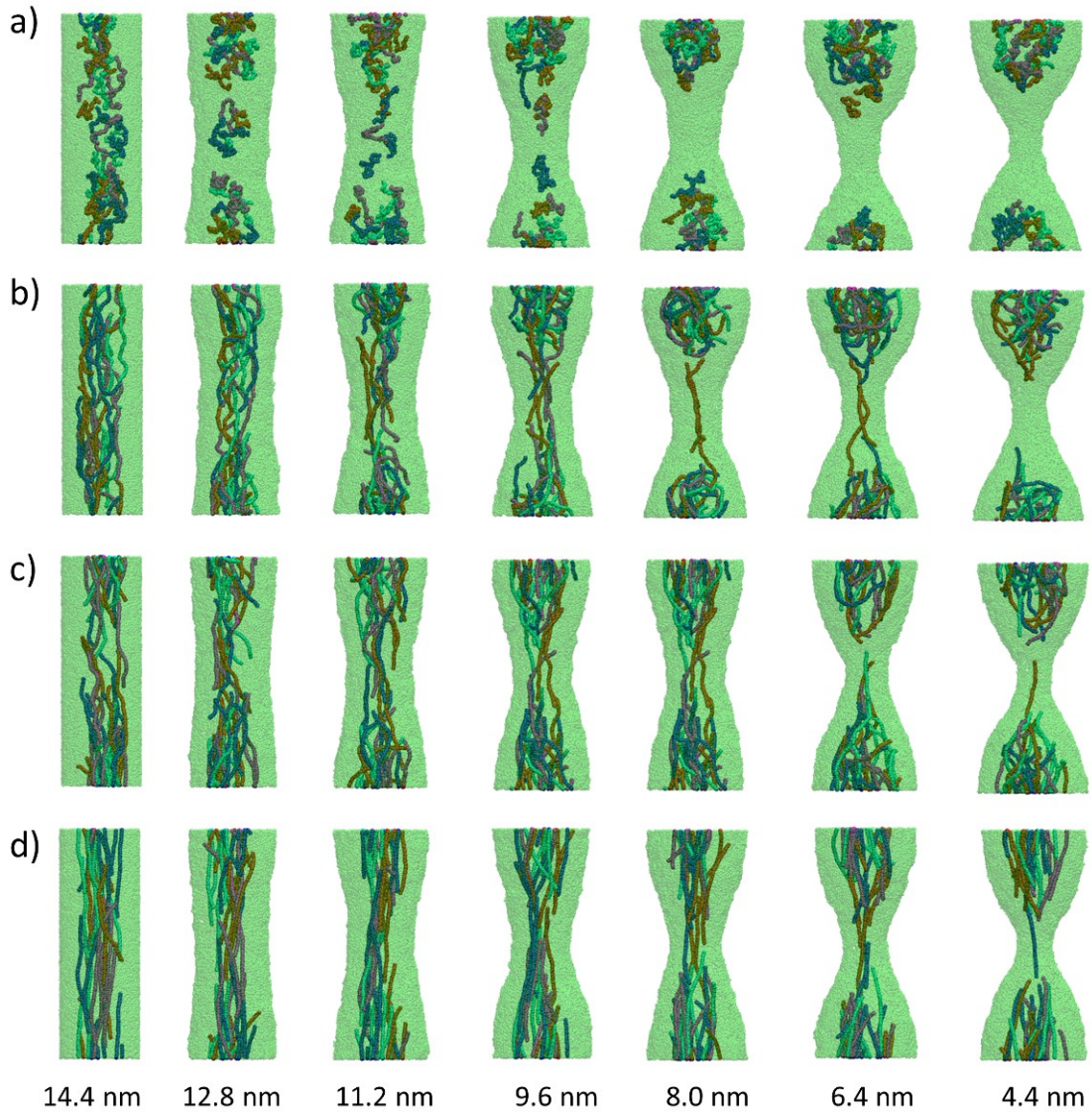

Fig. S13 Typical snapshots depicting the enforced pearling of nanotubes confining polymers of L = 43.75 nm and different bending stiffness. K = 1 (a), K = 10 (b), K = 20 (c), and K = 100 (d).

Table S1 The calculated persistence length of polymers of L = 43.75 nm with different values of K.

K	1	10	20	100
L_P (nm)	2.39	17.35	26.33	39.57

Table S2 The calculated persistence length of polymers of L = 87.5 nm with different values of K.

K	1	2	3	4	5	6
L_P (nm)	2.59	4.41	6.00	7.96	9.18	11.31
K	7	8	9	10	20	100
L_P (nm)	12.95	15.30	17.07	18.54	34.43	71.24